Articles

Cadmium Sulfide Nanoparticle Synthesis in Dps Protein from *Listeria innocua*

Kenji Iwahori,[†] Takahiro Enomoto,[‡] Hirotoshi Furusho,[‡] Atsushi Miura,[‡] Kazuaki Nishio,[§] Yumiko Mishima,[†] and Ichiro Yamashita*[,†,‡,§]

CREST, Japan Science and Technology Agency, 4-1-8 Honcho, Kawaguchi, Saitama, Japan, Nara Institute of Science and Technology, 8916-5 Takayama, Ikoma, Nara, 630-0101, Japan, Advanced Technology Research Laboratories, Matsushita Electronic Industrial Co., Ltd., 3-4 Hikaridai, Seika, Kyoto, Japan

Received December 5, 2006. Revised Manuscript Received April 6, 2007

Cadmium sulfide (CdS) nanoparticles (NPs) were synthesized in the cavity of the recombinant Dps cage-shaped protein from *Listeria innocua* (rLiDps) modifying the slow chemical reaction synthesis (SCRY) and two-step synthesis protocol (TSSP). The SCRY is realized by stabilizing cadmium ions as tetraamminecadmium and employing thioacetic acid (which is added in the final stage of the TSSP). The optimized condition produced cubic CdS NPs in the rLiDps cavity with an average diameter of 4.2 nm and small size dispersion. These CdS NPs showed photoluminescence. It was also found that the pH of the reaction solution affects the elemental composition CdS NPs. At pH 4.5 and 6.5, Cd_xS_y ($x < y$) NPs were obtained, and at pH 8.5, cubic CdS NPs were synthesized at pH 8.5.

Introduction

The nanoparticle (NP) is one of the most important components in nanotechnology. Many researchers have been developing a wide variety of methods for NP synthesis and have been studying the properties originated from the nanometric sizes of NPs. Presently, various kinds of NPs are routinely synthesized by chemical and physical methods. Recently, a biological method using protein cages as the biotemplate for the synthesis of metal and semiconductor NPs has become used for NP synthesis. Since the biotemplate works as a restricted nanomold and spatially constrains the growth of NPs, the obtained NPs are theoretically the same size and shape. This characteristic of "homogeneity" makes the biotemplate method very attractive because many applications need such size-controlled NPs. A nanoelectric device, which uses size-controlled conductive or semiconductive NPs as quantum dots (QD), is one such application.[1,2] The electron energy levels of QDs are quantized strongly according to the QD size, and homogeneity of the NP is crucial.

Many preceding works utilizing a biotemplate employed apoferritin from horse spleen (HsAFr)[3−15] (Figure 1A). HsAFr is a semispherical protein shell with an outer diameter of 12 nm and inner cavity of 7 nm. So far, several kinds of metal, metal oxide, and sulfic compound NPs have been synthesized, but reports on compound semiconductor NPs are rare. Recently, we designed a slow chemical reaction system (SCRY) and a two-step synthesis protocol (TSSP) to synthesize compound semiconductor NPs in the cavity of HsAFr and its genetic derivatives. The combination of the SCRY and TSSP worked well, and uniform 7 nm diameter semiconductor NPs (CdSe, ZnSe, and CdS) were successfully fabricated in the HsAFr and recombinant apoferritin.[16−20] From the point of view of electronic device applications, a

* To whom correspondence should be addressed. Tel: +81-743-72-6196. Fax: +81-743-72-6196. E-mail: ichiro@ms.naist.jp

[†] CREST.

[‡] Nara Institute of Science and Technology.

[§] Matsushita Electronic Industrial Co., Ltd.

(1) Miura, A.; Hikono, T.; Matsumura, T.; Yano, H.; Hatayama, T.; Uraoka, Y.; Fuyuki, T.; Yoshii, S.; Yamashita, I. *Jpn. J. Appl. Phys.* **2006**, *45*, L1.

(2) Hikono, T.; Matsumura, T.; Miura, A.; Uraoka, Y.; Fuyuki, T.; Takeguchi, M.; Yoshii, S.; Yamashita, I. *Appl. Phys. Lett.* **2006**, *88*, 023108.

(3) Meldrum, C. F.; Wade, J. V.; Nimmo, L. D.; Heywood, R. B.; Mann, S. *Nature* **1991**, *349*, 684.

(4) Meldrum, C. F.; Heywood, R. B.; Mann, S. *Science* **1992**, *257*, 522.

(5) Mann, S. *Nature* **1993**, *365*, 499.

(6) Douglas, T.; Dickson, D. P. E.; Betteridge, S.; Charnock, J.; Garner, C. D.; Mann, S. *Science* **1995**, *269*, 54.

(7) Meldrum, C. F.; Douglas, T.; Levi, S.; Arosio, P.; Mann, S. *J. Inorg. Biochem.* **1995**, *58*, 59.

(8) Wong, K. K. W.; Mann, S. *Adv. Mater.* **1996**, *8*, 928.

(9) Douglas, T.; Stark, T. V. *Inorg. Chem.* **2000**, *39*, 1828.

(10) Okuda, M.; Iwahori, K.; Yamashita, I.; Yoshimura, H. *Biotechnol. Bioeng.* **2003**, *84*, 187.

(11) Ueno, T.; Suzuki, M.; Goto, T.; Matsumoto, T.; Nagayama, K.; Watanabe, Y. *Angew. Chem., Int. Ed.* **2004**, *43*, 2527.

(12) Kramer, R. M.; Li, C.; Carter, D. C.; Stone, M. O.; Naik, R. R. *J. Am. Chem. Soc.* **2004**, *126*, 13282.

(13) Tsukamoto, R.; Iwahori, K.; Muraoka, M.; Yamashita, I. *Bull. Chem. Soc. Jpn.* **2005**, *78*, 2075.

(14) Kim, J.-W.; Choi, S. H.; Lillehei, P. T.; Chu, S.-H.; King, G. C.; Watt, G. D. *Chem. Commun.* **2005**, 4101.

(15) Okuda, M.; Kobayashi, Y.; Suzuki, K.; Sonoda, K.; Kondoh, T.; Wagawa, A.; Kondo, A.; Yoshimura, H. *Nano lett.* **2005**, *5*, 991.

(16) Yamashita, I.; Hayashi, J.; Hara, M. *Chem. Lett.* **2004**, *33*, 1158.

10.1021/cm0628799 CCC: $37.00
Published on Web 06/02/2007

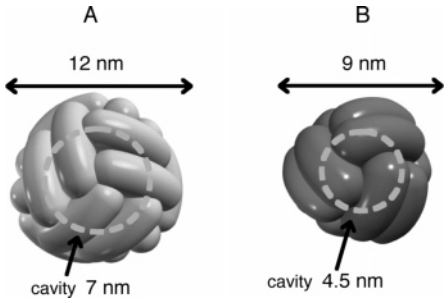

Figure 1. Schematic drawing of apoferritin from horse spleen (HsAFr) and Dps protein from *Listeria innocua* (LiDps). The inner diameter of HsAfr (A) and LiDps (B) is 7 and 4.5 nm, respectively.

smaller QD is more preferable. A smaller QD has a bigger electron energy split, which can make quantum electronic devices operate at higher temperature and more stably. Biotemplated synthesis of a semiconductor NP smaller than 7 nm should therefore be addressed. A few reports used a smaller cage-shaped protein, Dps cage-shaped protein is from *Listeria innocua* (LiDps), for synthesis of a metal oxide NP. LiDps is composed of 12 identical 18 kDa subunits, which has an outer diameter of 9 nm and an inner diameter of 4.5 nm (Figure 1B). This small cage structure of LiDps has hydrophilic channels on a threefold axis (a threefold channel), through which iron ions enter, and about 500 iron atoms are stored as a ferric oxyhydroxide NP. The threefold channels contain negatively charged amino acids, such as aspartic acids.[21−23] There are only two reports describing NP synthesis in the LiDps cavity.[24,25] The cavity volume is approximately a quarter of that of the HsAFr. If semiconductor NPs could be synthesized in this LiDps cavity, homogeneous QDs with diameter of 4.5 nm would be obtained. However, the mechanism of biomineralization of LiDps is not yet clear, so some cutting-edge research on the mechanism is necessary.

In this paper, we report synthesis of small CdS NPs in the LiDps cavity. We overproduced recombinant apo-Listeria Dps (rLiDps) and applied the SCRY and TSSP methods, which are theoretically effective for one-pod synthesis of CdS NPs in rLiDps, and we modified the synthesis conditions on the basis of the experimental results. The modification made it possible to fabricate 4.2 nm diameter fluorescent CdS NPs in the rLiDps cavity. The effect of the pH of the reaction solution on the elemental composition of the synthesized NP is also discussed.

(17) Iwahori, K.; Yoshizawa, K.; Muraoka, M.; Yamashita, I. *Inorg. Chem.* **2005**, *44*, 6393.
(18) Iwahori, K.; Morioka, T.; Yamashita, I. *Phys. Stat. Sol. (a)* **2006**, *203*, 2658.
(19) Iwahori, K.; Yamashita, I., submitted.
(20) Iwahori, K.; Yamashita, I., *Journal of Physics*: *Conference Series* **2007**, *61*, 492.
(21) Bozzi, M.; Mignogna, G.; Stefanini, S.; Barra, D.; Longhi, C.; Valenti, P.; Chianocone, E. *J. Biol. Chem.* **1997**, *272*, 3259.
(22) Ilari, A.; Stefanini, S.; Chiancone, E.; Tsernoglou, D. *Nat. Struct. Biol.* **2000**, *7*, 38.
(23) Su, M.; Cavallo, S.; Stefanini, S.; Chianocone, E.; Chasteen, N. D. *Biochemistry* **2005**, *44*, 5572.
(24) Allen, M.; Willits, D.; Mosolf, J.; Young, M.; Douglas, T. *Adv. Mater.* **2002**, *14*, 1562.
(25) Allen, M.; Willits, D.; Young, M.; Douglas, T. *Inorg. Chem.* **2003**, *42*, 6300.

Experimental Section

Construction and Purification of rLiDps. We reconstructed a recombinant apoferritin of *Listeria inocua*. The gene-coded full-length amino acids (1−175) of rLiDps[25] from pET30a plasmid digested an EcoRI-Hind III site and cloned into the pMK-2 plasmid (pLIT). This pLIT plasmid transformed into Novablue competent cells (Novagen).

The Novablue with pLIT was cultured in 3 L of LB medium with ampicillin (100 mg/mL) at 37 °C for 16 h. After cultivation, mutant cells were harvested by centrifugation and were resuspended in 15 mL of 50 mM Tris-HCl buffer (pH 8.0). The suspension was then disrupted by ultrasonic oscillation (SONIFER 250, Branson) in an ice bath for 2 min, and this procedure was repeated three or four times. Cell debris was removed by centrifugation at 10 000 rpm for 20 min, and the supernatant was treated at 65 °C for 20 min to denature impurities. The solution was centrifuged again, and the supernatant was applied to a Q-sepharose HP column (2.0 × 10 cm, Amersham Biosciences) equilibrated with 50 mM Tris-HCl buffer (pH 8.0). The rLiDps was eluted with 50 mM Tris-HCl buffer with a linear NaCl gradient from 0 to 500 mM at an elution rate 2.0 mL/min. The fractions containing recombinant apoferritin were collected. The solution was concentrated and purified by a Sephacryl S-300 (2.6 × 60 cm, Amersham Biosciences) gel-filtration column chromatography equilibrated with 50 mM Tris-HCl buffer with 150 mM NaCl (pH 8.0). To check the purity of the obtained monomeric 12-subunits rLiDps, each eluted fraction from the Sepahcryl S-300 column chromatography was analyzed by gel filtration column chromatography, namely, TSK-GEL BIOASSIST G4SWXL (TOSOH, Japan). The monomeric rLiDps fractions after leaving the Sepahcryl S-300 column chromatography were collected and were used to fabricate CdS NP cores.

Cadmium Sulfide Mineralization to Cavity of rLiDps. The basic solutions include 0.3 mg/mL rLiDps, 40 mM ammonium acetate, and 1 mM cadmium acetate. An ammonia water up to 150 mM and thioacetic acid up to 10 mM were added in the final step to the basic solution. The reaction mixture was kept overnight at room temperature, and a small fraction was observed by transmission electron microscopy (TEM) when necessary. After overnight reaction, the solution including rLiDps with an NP core was centrifuged at 12 000 rpm for 10 min to remove bulk precipitates. The solution was then replaced with 150 mM NaCl by repetitive concentration (Centriprep 75, Amicon, Danvers MA) and addition of 150 mM NaCl. The solution was applied to a gel filtration column (TSK-GEL BIOASSIST G4SWXL, TOSOH, Japan) equilibrated with 150 mM NaCl, and the eluted fraction including rLiDps with an NP core was collected and condensed (Centriprep 75, Amicon, Danvers, MA). The purified rLiDps with CdS NP cores (CdS-rLiDps) was used for all experiments.

Transmission Electron Microscopy (TEM) and Energy-Dispersive Spectra Analysis (EDS) of NP Cores Synthesized in rLiDps. Formation of CdS NP cores was observed by TEM (JEM-2200FS, JEOL, JAPAN). Several microliters of CdS-rLiDps were put on a carbon film coated mesh, and excessive solution was removed. CdS-rLiDps was stained with 1% aurothioglucose (Wako Pure Chemical Industries, Ltd, Japan), which was already confirmed not to stain the rLiDps cavity. After drying of the mesh with rLiDps in ambient air, TEM observation of the mesh with rLiDps was carried out. The NP core sizes were measured using the TEM images digitized at a resolution of 0.3 nm and were analyzed on a PC using software (Ryushi-Kaiseki, Sumitomo Material Industry, Japan). High-resolution TEM images of the NP cores were taken by TEM (JEM-3100FEF, JEOL, Japan) without stain of 1% aurothioglucose. The acceleration voltage on the TEM is 300 keV.

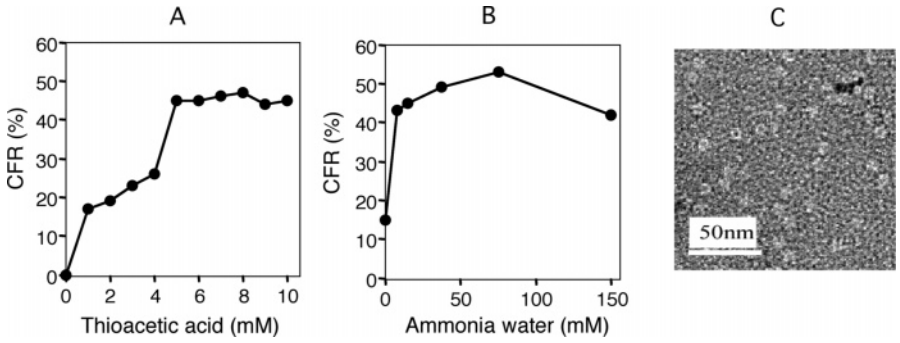

Figure 2. Effects of thioacetic acid and ammonia water on CFR of CdS NP synthesis in an rLiDps cavity. The effect of thioacetic acid (A) and the effect of ammonia water (B) on the CFR were calculated from TEM images. (C) A TEM image of CdS NP cores synthesized in the optimized reaction solution including 0.3 mg/mL rLiDps, 40 mM ammonia acetate, 75 mM ammonia water, 1 mM cadmium acetate, and 5 mM thioacetic acid.

EDS analysis was performed using the same sample. EDS measurement standard is Al Kα (1.49 eV) and Cu Kα (8.05 eV).

Photoluminescence (PL) Analysis of rLiDps with NP Core. Four hundred microliters of CdS-rLiDps adjusted to 2.5 mg/mL in quartz cells was irradiated by UV-light maximum peaks at 310 nm (Epi-Light FA500, AISIN, TAITEC, Japan), and the photoluminescence (PL) was observed. The PL spectra were measured by spectrofluorophotometer (RF 5300C, Shimadzu, Japan).

X-ray Diffraction (XRD) Measurement. A total of more than 50 mg CdS-rLiDps was purified by HPLC with a gel-filtration column (TSK-GEL BIOASSIST G4SWXL, TOSOH, Japan). The solution including the complete rLiDps and rLiDps with NP core was centrifuged by high-speed centrifugation (120 000*g*). The pellet after centrifugation was intensively washed with pure water by repetitive suspension and centrifugation. It was then nitrogen-gas dried and was gently ground using a mortar. XRD measurements were carried out with an X-ray generator (RINT2500/PC; Rigaku Corp., Tokyo, Japan) operated at 50 kV and 200 mA with a copper target.

Results and Discussion

Optimization of CdS NP Synthesis in the rLiDps Cavity. In the previous study, we demonstrated that the combination of the SCRY and TSSP can synthesize a 7 nm diameter CdS NP in the HsAFr cavity by one-pot synthesis.[19,20] The optimized reaction solution in the study is 0.3 mg/mL HsAFr, 40 mM ammonia acetate, 75 mM ammonia water, 1 mM cadmium acetate, and 1 mM thioacetic acid. The three key results of the previous study were as follows: (1) a high concentration of ammonium ions compared to cadmium concentration to stabilize cadmium ions as tetraamminecadmium ions; (2) slow supply of sulfide ions into the reaction solution; and (3) the addition of S source must be the final step. The repression of fast reaction between cadmium and sulfur sources by the stabilization of cadmium ions and the slow supply of sulfur sources lead to the repression of the bulk precipitation in the reaction solution drastically. The stabilized cadmium ions were quickly accumulated in the cavity because of the negative electronic potential inside the cavity. Thioacetic acid (which was added in the final step) slowly delivered sulfur sources, which reacted preferentially with the condensed cadmium ions in the cavity.

To synthesize a CdS NP smaller than 7 nm, we used the same condition of the reaction solution to synthesize CdS NP in the HsAFr. The reaction solution for the synthesis including 0.3 mg/mL rLiDps, 40 mM ammonia acetate, 75 mM ammonia water, 1 mM cadmium acetate, and 1 mM thioacetic acid at pH 6.5 was incubated overnight. The CdS core formation ratio (CFR) of CdS NP core synthesized in the rLiDps was found to be about 16%, which is much lower than that of HsAFr. The CFR was calculated by dividing the number of core-containing rLiDps (including CdS and Cd_xS_y) by the number of all rLiDps in TEM images. This result suggests that the behavior of CdS biomineralization of rLiDps is different from that of HsAFr. The low CFR may be due to the difference between the CdS nucleation or the growth rate in the cavity in the cases of rLiDps and HsAFr. For the one-pot synthesis of CdS NP in the protein shell, the supplies of cadmium ion and sulfur source are critical. The supply of source ions has to keep pace with the CdS nucleation and growth in the protein shell. Since cadmium ions are stabilized by excessive ammonia water, the supply speed of sulfur source in the reaction solution is mainly determined by the speed degradation of thioacetic acid. Therefore, by changing the concentration of thioacetic acid, we first determined the optimum supply speed of sulfur source. Solutions including the basic solution (0.3 mg/mL rLiDps, 40 mM ammonia acetate, 1 mM cadmium acetate) and 7.5 mM ammonia water were prepared, and up to 10 mM of thioacetic acid was added. The solution pH became around 9.0 by adding ammonia water. Therefore, the solution pH was adjusted by acetic acid to 6.5. Then, the solutions were left at room temperature for 24 h.

Thioacetic acid was decomposed slowly for a few days at pH 6.5,[19,20] and it was expected that sulfur source supply by the hour linearly would correspond to the thioacetic acid concentration. After the 24 h incubation, the reaction solution was observed by TEM, and CFR was calculated from the TEM images. Figure 2A shows the effect of the initial concentration of thioacetic acid on CFR, which increased in proportion to concentration of thioacetic acid up to 5 mM, after which it formed a plateau. Maximum CFR, 47%, was achieved at a concentration of 8 mM of thioacetic acid. However, yellow bulk precipitates increased in proportion to concentration of thioacetic acid of more than 5 mM. This result suggests that the nucleation and growth rate of CdS increased outside the rLiDps cavity. Given the fact that the CFR of over 5 mM is similar to that of 5 mM, increased amount of sulfur source per hour up to 5 mM is favorable, but more than 5 mM is harmful, because of production of

unnecessary bulk precipitates of cadmium and sulfur. We concluded that a concentration of 5 mM of thioacetic acid is suitable for the synthesis of CdS NP core in the rLiDps. This concentration is higher than that in the case of HsAFr (i.e., 1 mM), and sulfur source supply rate is much higher. This result indicates that the nucleation and growth of CdS NP core in the rLiDps cavity is faster than that in the HsAFr cavity. It is therefore reasonable that 5 mM of thioacetic acid is needed to synthesize a CdS NP in the rLiDps cavity.

As mentioned above, in SCRY, ammonium ions stabilize cadmium ions as tetraamminecadmium ions. However, free cadmium ion concentration is determined by chemical equilibrium and, actually, the concentration of ammonia water slightly affects CFR. We surveyed the effect of the ammonia water on CdS NP synthesis in the rLiDps cavity for the safety. The basic solution and 5 mM thioacetate were prepared, and up to 150 mM of ammonia water was added. The solution pH was adjusted to 6.5, and the reaction solutions were left at room temperature for 24 h. Figure 2B shows the effect of ammonia water on the CFR of the rLiDps with NP cores. In the without ammonia water case, CFR is low because of the fast NP-core formation in the bulk solution. The effect of ammonia water is clear, and CFR increases up to 75 mM ammonia water and peaks at 53%. The color of the reaction solution less than 75 mM ammonia water became a little turbid after 24 h incubation. That is, the ammonia water with lower concentration still has a little bulk precipitate. On the other hand, the reaction solution with over 75 mM ammonia water stayed clear yellow, and the precipitates are scarce. However, 150 mM ammonia water caused overprotection of cadmium ions, and free cadmium ions were too few to form a CdS NP in the cavity during 24 h incubation, so CFR decreased. The higher ammonia water concentration therefore needs the longer incubation time. On the whole, the ammonia water concentration is not so crucial, and at least there was excessive compared to cadmium ions. We thus selected an ammonia water concentration of 75 mM, namely, the same value as in the HsAFr case.[19] CdS NP cores were synthesized in the optimized reaction solution including the basic solution, 75 mM ammonia water, and 5 mM thioacetic acid. This solution was adjusted to pH 6.5 by acetic acid. A typical TEM image of CdS NPs in the rLiDps cavity is shown in Figure 2C. The negatively stained TEM image shows dots surrounded by a protein shell. The optimization of the sulfur source and ammonia water produced CFR 3.3 times higher than the initial CFR, that is, 16%. Previous synthesis of CdSe NP in the HsAFr cavity by SCRY and TSSP was achieved more than 90% CFR for a few hours. On the other hand, the synthesis of CdS NP in the HsAFr cavity needed about 18 h. These data suggested a lower catalytic activity of CdS than that of CdSe NPs. It is likely that the low catalytic activity of CdS NP will affect the low CFR of rLiDps cavity. Perhaps, the small inner surface area of rLiDps cavity also causes the decrease of cadmium ion binding site in rLiDps cavity, which is 26 in the HsAFr cavity,[8] resulting in the lower CFR than that of CdSe.

To compare the catalytic activity of CdS NP in rLiDps and HsAFr cavity, we estimated the formation time of CdS NP in the rLiDps and HsAFr cavity by TEM observation. CdS NP in rLiDps was formed after about 12 h and CdS NP in HsAFr was formed after about 18 h (supporting figure). These data indicate that the formation of CdS NP in rLiDps cavity is higher than that of HsAFr cavity. These results are explained as follows. The total capacity of rLiDps cavity in the reaction solution is about 1/40 000 of the bulk solution. This indicates that the synthesis rate in rLiDps cavity is at least 40 000 times faster than that of the bulk solution. On the other hand, total capacity of HsAFr cavity in the reaction solution is about 1/20 000 of the bulk solution.[17] It is one-half of rLiDps. Therefore, it is likely that the rate of CdS NP synthesis in rLiDps cavity will be faster than the HsAfr cavity.

Effect of Reaction Solution pH on the CdS-rLiDps Synthesis. The NPs synthesized using the optimized reaction solution at pH 6.5 were analyzed by energy-dispersive spectra analysis (EDS). Unexpectedly, EDS shows the element ratio was 2:3 for cadmium to sulfur. Moreover, the synthesized CdS NPs showed no photoluminescence (excited by UV light with 310 nm maximum peak). These results are quite different from the case of HsAFr, where fluorescent CdS NPs were successfully produced.[19] Thioacetic acid degrades to H_2S, HS^-, or S^{2-} according to solution pH, which is given as follows.

$$CH_3COSH + H_2O \rightarrow CH_3COOH + H_2S \quad (1)$$

$$H_2S \rightarrow HS^- + H^+ \qquad pK_a = 7.0 \quad (2)$$

$$HS^- \rightarrow S^{2-} + H^+ \qquad pK_a = 13.9 \quad (3)$$

Under an acidic condition, H_2S is released into the reaction solution. Under the alkaline condition, H_2S is further decomposed into HS^- and S^{2-} according to the pH. H_2S, HS^-, and S^{2-} have the ability to react with Cd^{2+} and make CdS. However, in the case of HS^- and S^{2-}, at the threefold channel, there is an electrostatic potential barrier that has negatively charged amino acids. The barrier heights are different according to the charge of sulfur sources.

To address this idea, we synthesized NP cores in three different pH solutions of the optimized reaction solution. Each reaction solution was adjusted by acetic acid to pH 4.5, 6.5, and 8.5. All solutions changed color slowly from light yellow to golden yellow. Bulk precipitates were observed in reaction solutions with pH 4.5 and 6.5 after 24 h but were not observed in the pH 8.5 solution. This result indicates that the acidic reaction solution produced precipitates. In the acidic solution, H_2S is the major sulfur source and volatilizes in the reaction solution. It indicates that the supply rate of H_2S is larger than the consumption rate by the NP synthesis in the rLiDps cavity, and excess H_2S in the solution reacts with free cadmium ions to produce bulk precipitate outside the protein shell. In the case of pH 4.5, the precipitation increased in quantity, so we added 150 mM NaCl to prevent the bulk precipitate composed from rLiDps and H_2S.

Figure 3 shows TEM images of NP cores synthesized at pH 4.5 (A), pH 6.5 (B), and pH 8.5 (C) after 24 h incubation. NP cores were formed under all conditions. Figure 3D shows

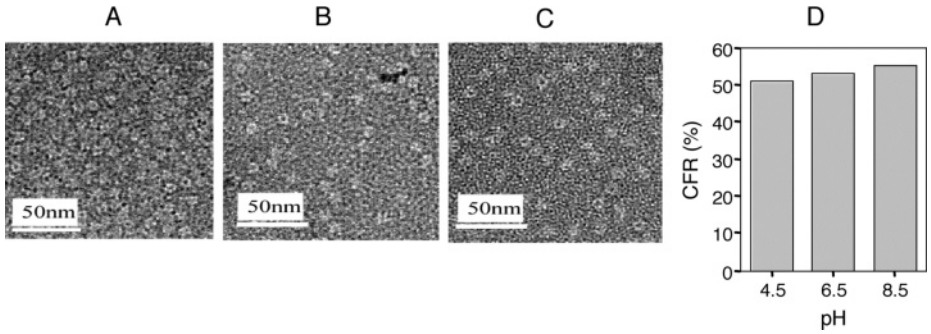

Figure 3. TEM images of each diluted sample observed by using appropriate deionized water. TEM images of NP cores in the rLiDps synthesized in the optimized reaction solutions with different pH 4.5 (A), pH 6.5 (B), and pH 8.5 (C). (D) Plot of CFRs of NPs synthesized in the solution with different solution pH.

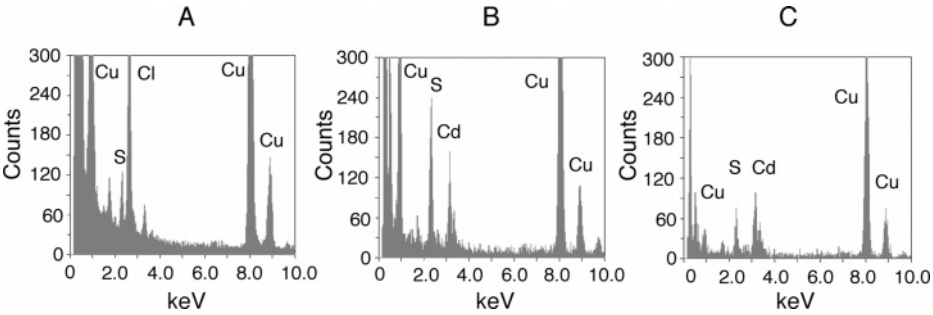

Figure 4. EDS spectra of NPs synthesized in the optimized reaction solution at pH 4.5 (A), pH 6.5 (B), and pH 8.5 (C). At pH 4.5, Kα of chlorine (2.6 keV) and sodium (1.0 keV) come from NaCl in the solution. The copper peaks (0.9, 8.0, and 8.9 keV) and carbon peak (0.3 keV) are attributed to the TEM grid and protein shell. The peak at 3.3 keV is an artifact.

the CFR of rLiDps with NP cores synthesized under the three pH conditions. It is clear that CFR was maintained in the range from 51% to 55%. This result indicates that pH of the solution does not affect CFR.

Elemental compositions of the synthesized NP cores were analyzed by EDS. The EDS spectra showed both the Kα, Cd peak (3.1 keV) and Lα, S peak (2.2 keV) signals from NP cores synthesized at pH 6.5 and 8.5. However, the Kα, Cd peak was not observed clearly in the EDS spectrum at pH 4.5. Cadmium and sulfur composition ratio of the three cores calculated from the spectra are 1:9 for pH 4.5, 1:1.5 for pH 6.5, and 1:1 for pH 8.5 (Figure 4). The NPs synthesized in the rLiDps cavity at pH 4.5 and 6.5 consist of Cd_xS_y crystal, where $x = 0.1$ and $y = 0.9$ or $x = 2$ and $y = 3$, and CdS NP cores were only synthesized at pH 8.5. These data suggest that the pH of reaction can be shifted easily to the composition of synthesized NPs in the cavity. We selected the reaction pH at 8.5 for CdS NP synthesis, because it only synthesizes Cd_xS_y ($x = 1$ and $y = 1$) NP in the rLiDps cavity.

This elemental composition shift was supposed to come from the difference in the major form of the sulfur source in the reaction solution. From the pK_a of H_2S degradation (eqs 2 and 3), H_2S is a major sulfur source at pH 4.5 and 6.5, and the HS^- is a major sulfur source with a very small amount of S^{2-} at pH 8.5. H_2S, HS^-, and S^{2-} exhibit different electrostatic barriers when they go through the threefold channel, the surface of which is composed of acidic amino acids. Neutral H_2S molecules can therefore go through easily and react with cadmium ions or the NP surface in the cavity, resulting in Cd_xS_y ($x < y$). However, HS^- and S^{2-} have an electrostatic barrier at the threefold channel to overcome. Hence, the entrance flow rate is slowed down, and the sulfur source supply rate became appropriate for CdS NP synthesis. As a result, CdS can be formed at pH 8.5.

Since the isoelectronic point of rLiDps is about pH 5.0 from the measurement of zeta potentials of rLiDps,[26] the negative charge of the outer surface from amino acid residues affects cadmium ion concentration in the vicinity of rLiDps. It affects the elemental component shift of NP synthesized in the cavity. In the case of pH 4.5, the outer surface is positively charged in net. That is, cadmium ions are repelled by the electronisity of protein shell and find it hard to enter the cavity. On the other hand, at pH 8.5, the outer surface has a negative charge. Cadmium ions are attracted to the surface of rLiDps, and enough cadmium ions go through the channel and into the cavity. This surface change of rLiDps likely enhances the elemental component shift further. There is a possibility that the cadmium ion binds to the outside of rLiDps and that the bulk CdS NP forms in this condition. However, the total capacity of rLiDps cavity is about 1/40 000 of the bulk solution, indicating that the synthesis rate in rLiDps is at least 40 000 times faster than that in the bulk solution. Therefore, the formation of CdS NPs in the rLiDps cavity will be prior to the CdS mineralization on the outside under the reaction - condition at pH 8.5 which H_2S gas is less than other conditions.

XRD Measurement and HR-TEM Observation of CdS NP Cores Synthesized in a Solution at pH 8.5. To determine the crystal structure of the CdS NP core synthesized in the optimized reaction solution adjusted to pH 8.5, X-ray powder diffraction (XRD) analysis and HR-TEM

(26) Yamada, K.; Yoshii, S.; Kumagai, S.; Fujiwara I.; Nishio, K.; Okuda, M.; Matsukawa, N.; Yamashita, I. *Jpn. J. Appl. Phys.* **2006**, *45*, 4259.

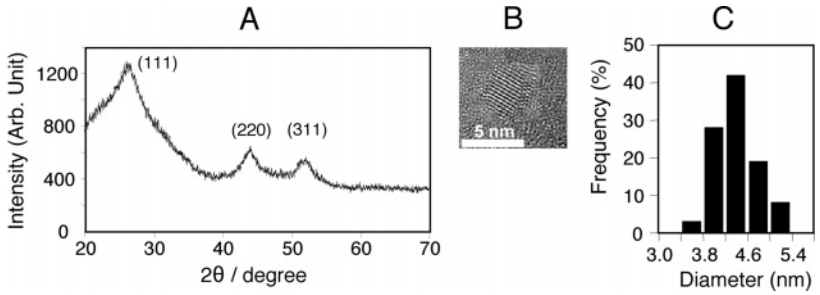

Figure 5. XRD pattern (A) and HR-TEM image (B) of CdS NP core synthesized in the optimized reaction solution adjusted at pH 8.5. The scale bar is 5 nm. A diameter distribution of synthesized CdS NPs at pH 8.5 (C).

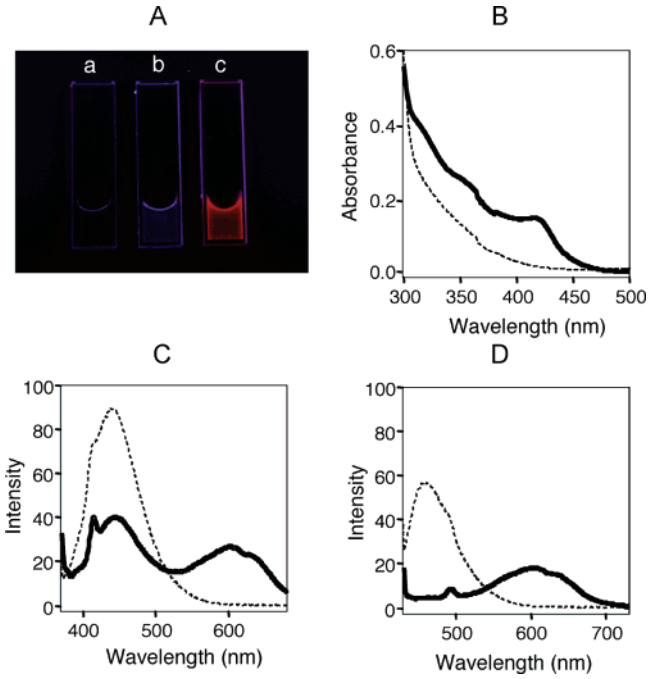

Figure 6. Photoluminescence (PL), absorption spectra, and PL spectra of rLiDps and rLiDps with CdS NP core synthesized at pH 8.5. (A) Images of PL of deionized water (a), rLiDps (b), and rLiDps with CdS NP core (c) were observed. (B) UV−vis absorption spectra of rLiDps (dashed line) and rLiDps with CdS NP core synthesized at pH 8.5 (solid line) and CdS-rLiDps synthesized at pH 8.5. The spectra were measured by a spectrophotometer. PL spectra of rLiDps (dashed line) and rLiDps with CdS NP core (solid line) were measured by an excitation at 360 nm (C) or 420 nm (D).

observation were carried out. The diffraction peaks were broad refracting from their nanometric size, but the peak positions were discernible. The set of peaks in the XRD data showed that the crystal structure of the CdS NP is cubic (Figure 5A). The half-peak width of the XRD spectra indicates that the crystalline domain is about 2−3 nm that is, smaller than the NP diameter and, hence, the obtained CdS NP cores are suggested to be polycrystalline. This conclusion is in agreement with the HR-TEM images (Figure 5B). These results suggest that the NP synthesis of CdS in the rLiDps cavity starts from the inner surface of the rLiDps cavity, as is the case with the CdS NP core in the HsAfr cavity.[19]

Genuine CdS NPs were synthesized in the optimized reaction solution at pH 8.5, and the NP size was measured from TEM images. The average size of the NP size is 4.2 ± 0.4 nm in diameter (Figure 5C). The diameter was calculated by software (Ryushi-kaiseki, Sumitomo Material Industry, Japan). This size was quite monodisperse, and this result is consistent with the interior size of the rLiDps. In addition, the diameter of CdS-rLiDps synthesized at pH 8.5 was measured by the dynamic light-scattering analysis. The protein cage of the unmineralized rLiDps is 9.4 nm in diameter, and the diameter of rLiDps with CdS NP is also 9.4 nm. There was no difference in the observed correlation function (data not shown). This result indicates that the protein cage remained intact during the synthesis of CdS NP, suggesting that all mineralization occurs in the protein cages.

Photoluminescence of CdS NPs in the rLiDps Cavity. The photoluminescence (PL) spectra of the rLiDps with NP cores synthesized in the reaction solution adjusted at pH 4.5, 6.5, and 8.5 were measured by a UV-lamp with 310 nm maximum peaks. The rLiDps with NP cores synthesized at pH 4.5 and 6.5 showed no PL spectra (data not shown). Only rLiDps with an NP core synthesized at pH 8.5 showed a red PL, although rLiDps without NP core shows a weak blue PL (Figure 6A). Absorption spectra and PL spectra of the rLiDps with CdS NP cores have three peaks, namely, 320, 360, and 420 nm (Figure 6B). Since the peak at 320 nm is due to protein shells, we measured the PL spectra of rLiDps and rLiDps with CdS NP cores using excitation light with wavelength of 360 nm (Figure 6C) and 420 nm (Figure 6D). Raman scattering of water is seen around 410 nm in Figure 6C. The PL peaks around 600 nm in both cases are due to bulk CdS NPs. This result is consistent with the analysis that synthesized NP in the rLiDps at pH 8.5 is cubic CdS NP. Both peaks at 440 and 460 nm from rLiDps decreased in the rLiDps with CdS NPs (Figure 6C and D), suggesting that there is a possibility that energy is lost in the protein shell's PL. It then transfers to and enhances the PL around 600 nm. The same phenomenon was observed in the CdS NPs synthesized in the HsAFr cavity.[19]

Conclusions

The first synthesis of semiconductor NPs by using a biotemplate, Dps cage-shaped protein from *Listeria innocua*, was performed. CdS NP cores were synthesized in a small cavity of the rLiDps by using the optimized reaction solution adjusted to pH 8.5 including 0.3 mg/mL rLiDps, 40 mM ammonia acetate, 75 mM ammonia water, 1 mM cadmium acetate, and 5 mM thioacetic acid. Keeping the reaction solution at pH 8.5 produced cubic crystalline CdS NP with diameter of 4.2 nm. The obtained CdS NPs showed a red PL.

The growth mechanism of CdS in the rLiDps cavity was compared with that of HsAFr. It is suggested that the catalytic activity of the inner surface of the rLiDps cavity can be higher or that the threefold channel has a structure allowing higher flow rate. The elemental shift of NPs synthesized at different pH is considered to be due to electrostatic interaction. That is, (1) Cd^{2+} ions are attracted or repelled depending on the net outer-surface charge of rLiDps, and (2) the incurrent of sulfur source to the rLiDps cavity is affected by the energy barrier originated between negatively charged threefold channel and a charge of sulfur source. This theory explains the elemental component shift of the NP by the reaction solution pH.

Our proposed slow chemical reaction system (SCRY) and two-step synthesis protocol (TSSP) are proven to be applicable to not only the synthesis of semiconductor NPs (CdSe, ZnSe, and CdS) in HsAFr but also to synthesis of CdS in rLiDps. We believe that the combination of SCRY and TSSP will be applicable to other semiconductor NPs such as Au_2S, ZnS and PbS in protein cages, though further experiments are necessary to understand the mechanism of semiconductors in the cage-shaped protein.

Acknowledgment. We wish to thank Prof. Trevor Douglas of Montana State University for providing a plasmid of Dps protein from *Listeria innocua*. This study is supported by the Core Research for Evolutional Science and Technology, Japan Science and Technology Agency.

Supporting Information Available: Plot of core formation ratios over time. This material is available free of charge via the Internet at http://pubs.acs.org.

CM0628799